Quantifying climate feedbacks in the middle atmosphere using WACCM

Maartje Sanne Kuilman[1], Qiong Zhang[2], Ming Cai[3], Qin Wen[1,4]

1. Department of Meteorology and Bolin Centre for Climate Research, Stockholm University, Stockholm, Sweden
2. Department of Physical Geography and Bolin Centre for Climate Research, Stockholm University, Stockholm, Sweden
3. Department of Earth, Ocean and Atmospheric Science, Florida State University, Tallahassee, Florida, USA
4. Laboratory for Climate and Ocean-Atmosphere Studies (LaCOAS), Department of Atmospheric and Oceanic Sciences, School of Physics, Peking University, Beijing, China

Corresponding author: Maartje Sanne Kuilman (maartje.kuilman@misu.su.se)

Key points:

- In a double CO_2 climate, the direct forcing of CO_2 would lead to a cooling which increases with increasing height in the middle atmosphere, with the cooling in the upper stratosphere about three times as strong as in the lower stratosphere.

- The ozone feedback yields a radiative feedback that generally mitigates this cooling. The dynamical feedback is another important feedback with large effects locally, while the effects of the water vapour feedback and especially the cloud and albedo feedbacks are only of importance in the lower stratosphere.

- CFRAM is very powerful tool to study climate feedbacks in the middle atmosphere however, there is an error term caused by the linearization in the method.

Abstract

The importance of the middle atmosphere for surface and tropospheric climate is increasingly realized. In this study, we aim at a better understanding of climate feedbacks in response to a doubling of CO_2 in the middle atmosphere using the climate feedback response analysis method (CFRAM). This method allows one to calculate the partial temperature changes due to an external forcing and climate feedbacks in the atmosphere. It has the unique feature of additivity, such that these partial temperature changes are linearly addable. We find that the temperature change due to the direct forcing of CO_2 increases with increasing height in the middle atmosphere, with the cooling in the upper stratosphere about three times as strong as in the lower stratosphere. The ozone feedback yields a radiative feedback that generally mitigates this cooling, however in the tropical lower stratosphere and in some regions of the mesosphere, the ozone feedback cools these regions further. The temperature response due to dynamical feedbacks is small in global average, although the temperature changes due to the dynamical feedbacks are large locally. The temperature change in the lower stratosphere is influenced by the water vapour feedback and to a lesser degree by the cloud and albedo feedback, while these feedbacks play no role in the upper stratosphere and the mesosphere. We find that the effects of the changed SSTs on the middle atmosphere are relatively small as compared to the effects of changing the CO_2. However, the changes in SSTs are responsible for large temperature changes as a result of the dynamical feedbacks and the temperature response to the water vapour feedback in the lower stratosphere is almost solely due to changes in the SSTs. As CFRAM has not been applied to the middle atmosphere in this way, this study also serves to investigate the applicability as well as the limitations of this method. This work shows that CFRAM is a very powerful tool to study climate feedbacks in the middle atmosphere. However, it should be noted that there is a relatively large error term associated with the current method in the middle atmosphere, which can be for a large part be explained by the linearization in the method.

1. Introduction

The middle atmosphere is the region of the atmosphere that encompassed the stratosphere, where the temperature increases with height, from 10-50 km and the mesosphere, where the temperature decreases with height, from about 50-90 km. A classic study by Manabe and Strickler (1964) shows that in the troposphere, water vapour is the dominant greenhouse gas, followed by CO_2. Ozone is responsible for the existence of the stratosphere and the reversal of the temperature gradient in the stratosphere.

The circulation in the troposphere is thermally driven, however this is quite different for the middle atmosphere. The air in the middle atmosphere is out of reach for convection and is not in direct contact with the Earth's surface, which means that the middle atmosphere is dynamically stable. In the absence of eddy motions the zonal-mean temperature would relax to a radiatively determined state. However, wave-driven motions of the air drive the state away from this state of radiative balance and in this way determine the heating and cooling patterns in the middle atmosphere (*Shepherd*, 2010).

Many chemical, physical and dynamical processes in the middle atmosphere are still often overlooked in climate model simulations. This can be noticed from the description of the experimental design in model intercomparison projects as in e.g. *Kageyama et al.* (2017) and *Taylor et al*. (2012). However, recently, there have been a number of studies that show the importance of the middle atmosphere for the surface and tropospheric climate. It has, for example, been shown that cold winters in Siberia are linked to changes in the stratospheric circulation (*Zhang et al.*, 2018).

Other studies show that the representation of ozone in climate models affects climate change projections (*Dietmüller et al.*, 2014; *Noda et al.,* 2017; *Nowack et al.*, 2015, 2018;). It has been found that the ozone representation can result in up to a 20% difference in simulated global mean surface warming (*Nowack et al.*, 2015), although the exact importance of changes in ozone seems to be dependent on both the model and the scenario (*Nowack et al*., 2015) and is not found by all studies (*Marsh et al.*, 2016).

Neglecting the effect of ozone may lead to a significant underestimation of the temperature during past climate if we compare with available paleoclimate reconstructions (*Ljungqvist et al*, 2019), and may also alter the future climate projections in different CO_2 scenarios. As the effect is found to be rather large in some studies, and absent in other, there is a need for a better understanding of the behaviour of the middle atmosphere in response to changing CO_2 conditions, as the ozone concentration is influenced by this.

Ozone is an example of a climate feedback, a process that changes in response to a change in CO_2-concentration and in turn dampens or amplifies the climate response to the CO_2 perturbation. These climate feedbacks are a challenging subject of study, as observed climate variations might not be in equilibrium, multiple processes are operating at the same time and moreover the geographical structures and timescales of different forcings differ. However, feedbacks form a crucial part of understanding the response of the atmosphere to changes in the CO_2-concentration.

Various methods have been developed to study these feedbacks, such as the partial radiative perturbation (PRP) method, the online feedback suppression approach and the radiative kernel method (*Bony et al.,* 2006 and the references therein). These methods study the origin of the global cimate sensitivity (Soden and Held, 2006; Caldwell et al., 2016; Rieger et al., 2017). The focus of these methods is on changes in the global mean surface temperature, global mean surface heat and global mean sensible heat fluxes (*Ramaswamy et al., 2019*).

These methods are powerful for this purpose; however, they are not suitable to explain temperature changes on spatially limited domains. They neglect non-radiative interactions between feedback processes and they only account for feedbacks that directly affect the radiation at the top of the atmosphere (TOA).

The climate feedback-response analysis method (CFRAM) is an alternative method which takes into account that the climate change is not only determined by the energy balance at the top of the atmosphere, but is also influenced by the energy flow within the Earth's system itself (*Cai and Lu, 2009, Lu and Cai*, 2009). The method is based on the energy balance in an atmosphere-surface column. It solves the linearized infrared radiation transfer model for the individual energy flux perturbations. This makes it possible to calculate the partial temperature changes due to an external forcing and these internal feedbacks in the atmosphere. It has the unique feature of additivity, such that these partial temperature changes are linearly addable.

As a practical diagnostic tool to analyse the role of various forcing and feedback, CFRAM has been used widely in climate change research on studying surface climate change (*Taylor et al.,* 2013; *Song and Zhang,* 2014; *Hu et al.,* 2017; *Zheng et al.,* 2019).

This method has been applied to study the middle atmosphere climate sensitivity as well (*Zhu et al.,* 2016). In Zhu et al. *(2016),* the CFRAM method has been adapted and applied to both model output, as well as observations. The atmospheric responses during solar maximum and minimum are studied and it is found that the variation in solar flux forms the largest radiative component of the middle atmosphere temperature response.

In the present work, we apply CFRAM to climate sensitivity experiments performed by the Whole Atmosphere Community Climate Model (WACCM), which is a high-top global climate system model, including the full middle atmosphere chemistry. We investigate the effects of doubling the CO_2-concentration and the accompanying sea surface temperature changes on the temperature changes in the middle atmosphere as compared to the pre-industrial state. We discuss the total responses and feedbacks, as well as those that are induced by doubling CO_2 and changes in the sea surface temperature and sea ice distribution separately.

2. The model and methods

2.1 Model description

The Whole Atmosphere Community Model (WACCM) is a chemistry-climate model, which spans the range of altitudes from the Earth's surface to about 140 km (*Marsh et al.,* 2013). The model consists of 66 vertical levels with irregular resolution, ~1.1 km in the troposphere above the boundary layer, 1.1–1.4 km in the lower stratosphere, 1.75 km at the stratosphere and 3.5 km above 65 km. The horizontal resolution is 1.9° latitude by 2.5° longitude.

WACCM is a superset of the Community Atmospheric Model version 4 (CAM4) developed at the National Center for Atmospheric Research (NCAR). Therefore, WACCM includes all the physical parameterizations of CAM4

(*Neale et al.,* 2013), and a well-resolved high-top middle atmosphere. The orographic gravity wave (GW) parameterization is based on *McFarlane* (1987). WACCM also includes parameterized non-orographic GWs, which are generated by frontal systems and convection (*Richter et al.,* 2010). The parameterization of non-orographic GW propagation is based on the formulation by *Lindzen* (1981).

The chemistry in WACCM is based on version 3 of the Model for Ozone and Related Chemical Tracers (MOZART). This model represents chemical and physical processes from the troposphere until the lower thermosphere. (*Kinnison et al.,* 2007). In addition, WACCM simulates chemical heating, molecular diffusion and ionization and gravity wave drag.

2.2 Experimental set-up

In this study, we first perform a simulation under pre-industrial conditions and take this experiment as a control run, forced with pre-industrial ocean surface conditions such as sea surface temperature and sea ice (referred to SSTs from now on), see table 1. The pre-industrial CO_2-concentration is set as 280 ppm, the SSTs are from the CMIP5 pre-industrial control simulation by the fully coupled earth system model CESM (*Hurrel et al.,* 2013). The atmosphere component of CESM is the same as WACCM, but does not include stratospheric chemistry.

We also run a perturbation experiment by doubling the CO_2 concentration to 560 ppm from pre-industrial level. In WACCM, the CO_2-concentration does not double everywhere in the atmosphere. Only the surface level CO_2 mixing ratio is doubled, and elsewhere in the atmosphere is calculated according to WACCM's chemical model. Other radiatively and chemically active gases, such as ozone, will change because of the changes in the CO_2-concentration, due to WACCM's chemical model as well.

For the double CO_2 simulation, we run two experiments by using two SSTs forcing, one is keeping the pre-industrial SSTs unchanged, and another one from a double CO_2 equilibrium simulation by CESM. To investigate the effect of SSTs, we further run a simulation for only using the SST forcing from the coupled CESM for double CO_2 condition, but keep the CO_2-concentration as 280 ppm. All the simulations are run for 50 years, of which the last 40 years are used for analysis.

Table 1. Set-up of the model experiments.

Experiment	**CO_2**	**SSTs from CESM equilibrum run**
Pre-industrial	280 ppm	PI control
CO_2 and SSTs high	560 ppm	Double CO2 run
CO_2 high	560 ppm	PI control
SSTs high	280 ppm	Double CO2 run

2.3 Climate feedback-response analysis method (CFRAM)

In this study, we aim to understand and quantify the different climate feedbacks that may play a role in the middle atmosphere in a high CO_2 climate. For this purpose, we apply a climate feedback-response analysis method (CFRAM).

As briefly discussed in the introduction, traditional methods to study climate feedbacks are based on the energy balance at the top of the atmosphere (TOA). This means that the only climate feedbacks that are taken into account are those that effect the radiative balance at the TOA. However, there are other thermodynamic and dynamical processes that do not directly affect the TOA energy balance, while they do yield a temperature response in the atmosphere.

Contrary to TOA-based methods, CFRAM considers all the radiative and non-radiative feedbacks that result from the climate system due to response to an external forcing. This means that CFRAM starts from a slightly different definition of a feedback process. Note also that as the changes in temperature are calculated simultaneously, the vertical mean temperature or lapse rate feedback per definition do not exist in CFRAM.

Another advantage of CFRAM is that it allows for measuring the magnitude of a certain feedback in units of temperature. We can actually calculate how much of the temperature change is due to which process. The *'climate response'* in the name of this method refers to the changes in temperature in response to the climate forcings and climate feedbacks.

The mathematical formulation of CFRAM is based on the conservation of total energy (*Lu and Cai*, 2009). At a given location in the atmosphere, the energy balance in an atmosphere-surface column can be written as:

$$\vec{R} = \vec{S} + \vec{Q}^{conv} + \vec{Q}^{turb} - \vec{D}^{v} - \vec{D}^{h} + \vec{W}^{fric} \qquad (1)$$

$\vec{R}$ represents the vertical profile of the net long-wave radiation emitted by the different layers in the atmosphere and surface. $\vec{S}$ is the vertical profile of the solar radiation, which is absorbed by these layers. $\vec{Q}^{turb}$ is the convergence of total energy in each layer due to turbulent motions, $\vec{Q}^{conv}$ is convergence of total energy into the layers due to convective motion. $\vec{D}^{v}$ is the large-scale vertical transport of energy from different layers to others. $\vec{D}^{h}$ is the large-scale horizontal transport within the layers and $\vec{W}^{fric}$ is the work done by atmospheric friction.

Due to an external forcing (in this study, the change in CO_2-concentration and/or change in SSTs), the difference in the energy flux terms then becomes:

$$\Delta\vec{R} = \Delta\vec{F}^{ext} + \Delta\vec{S} + \Delta\vec{Q}^{conv} + \Delta\vec{Q}^{turb} - \Delta\vec{D}^{v} - \Delta\vec{D}^{h} + \Delta\vec{W}^{fric} \qquad (2)$$

In which the delta (Δ) stands for the difference between the perturbation run and the control run.

CFRAM takes advantage of the fact that the infrared radiation is directly related to the temperatures in the entire column. The temperature changes in the equilibrium response to perturbations in the energy flux terms can be calculated. This is done by requiring that the temperature-induced changes in infrared radiation to balance the non-temperature induced energy flux perturbations.

Equation (2) can also be written as:

$$\Delta\big(\vec{S}-\vec{R}\big)_{total} + \Delta dyn = 0 \qquad (3)$$

The term $\Delta(\vec{S}-\vec{R})$ we can calculate as the longwave heating rate and the solar heating rate are output variables of the model simulations. We take the time mean of the WACCM data and perform the calculations for each grid point of the WACCM data. This means that in the end, we will have the temperature changes at each latitude, longitude and height.

We then calculate the difference in these heating rates for the perturbation simulation and the control simulation.

We use the term $\Delta\big(\vec{S}-\vec{R}\big)_{total}$ to calculate the dynamics term Δdyn.

$$\Delta dyn = -\Delta\big(\vec{S}-\vec{R}\big)_{total} \qquad (4)$$

WACCM provides us with a heating rate in Ks^{-1}. For the CFRAM calculations, we need the energy flux in Wm^{-2}. We can calculate the energy flux by multiplying with the mass of different layers in the atmosphere and the specific heat capacity.

$$\Delta(\vec{S}-\vec{R}) = \Delta(\vec{S}-\vec{R})_{(WACCM)} * mass_k * c_p \qquad (5)$$

In which $\Delta(\vec{S}-\vec{R})$ is the difference in the shortwave radiation $\overrightarrow{(S)}$ and longwave radiation $\overrightarrow{(R)})$ between the perturbation run and the control run as a flux in Wm^{-2}, while $\Delta(\vec{S}-\vec{R})_{(WACCM)}$ is this difference as heating rate in Ks^{-1} in WACCM, with $mass_k = \frac{p_{k+1}-p_k}{g}$ with p in Pa and $c_p = 1004 \;\; \mathrm{J}\, kg^{-1}\, K^{-1}$ the specific heat capacity at constant pressure.

WACCM includes a non-local thermal equilibrium (non-LTE) radiation scheme above 50 km. It consists of a long-wave radiation (LW) part and a short-wave radiation (SW) part which includes the extreme ultraviolet (EUV) heating rate, chemical potential heating rate, CO_2 near-infrared (NIR) heating rate, total auroral heating rate and non-EUV photolysis heating rate.
Therefore, we split the term $\Delta\big(\vec{S}-\vec{R}\big)_{total}$ in an LTE and a non-LTE term:

$$\Delta\big(\vec{S}-\vec{R}\big)_{total} = \Delta(\vec{S}-\vec{R})_{LTE} + \Delta(\vec{S}-\vec{R})_{non-LTE} \qquad (6)$$

WACCM provides us with the total longwave heating rate as well as the total solar heating rate and the non-LTE longwave and shortwave heating rates for the different runs. This means that we can calculate the term $\Delta(\vec{S}-\vec{R})_{non-LTE}$ as well, where we again need to convert our result from Ks^{-1} to Wm^{-2}:

$$\Delta(\vec{S}-\vec{R})_{non-LTE} = \Delta(\vec{S}-\vec{R})_{non-LTE(WACCM)}\ \ mass_k\ *\ c_p \qquad (7)$$

This term can be inserted in equation (3):

$$\Delta(\vec{S}-\vec{R})_{LTE} + \Delta(\vec{S}-\vec{R})_{non-LTE} + \Delta dyn = 0 \qquad (8)$$

The central step in CFRAM is to decompose the radiative flux vector, using a linear approximation.

We start by decomposing the LTE infrared radiative flux vector $\Delta\vec{R}$

$$\Delta\vec{R}_{LTE} = \frac{\partial\vec{R}}{\partial\vec{T}}\Delta T + \Delta\vec{R}_{CO_2} + \Delta\vec{R}_{O_3} + \Delta\vec{R}_{H_2O} + \Delta\vec{R}_{albedo} + \Delta\vec{R}_{cloud} \qquad (9)$$

where $\Delta\vec{R}_{CO_2}$, $\Delta\vec{R}_{O_3}$, $\Delta\vec{R}_{H_2O}$, $\Delta\vec{R}_{albedo}$, $\Delta\vec{R}_{cloud}$ are the changes in infrared radiative fluxes due to the changes in CO_2, ozone, water vapour, albedo and clouds, respectively.

For equation (9), we assumed that radiative perturbations can be linearized by neglecting the higher order terms of each thermodynamic feedback and the interactions between these feedbacks. This is also commonly done in the PRP method (*Bony et al.,* 2006).

The term $\frac{\partial\vec{R}}{\partial\vec{T}}\Delta T$ represents the changes in the IR radiative fluxes related to the temperature changes in the entire atmosphere-surface column. The matrix $\frac{\partial\vec{R}}{\partial\vec{T}}$ is the Planck feedback matrix, in which the vertical profiles of the changes in the divergence of radiative energy fluxes due to a temperature change are represented.

We calculate this feedback matrix using the output variables of the perturbation and the control run of WACCM and inserting these in the CFRAM radiation code: atmospheric temperature, surface temperature, reference height temperature, ozone, surface pressure, solar insolation, downwelling solar flux at the surface, net solar flux at the surface, dew point temperature, cloud fraction, cloud ice amount, cloud liquid amount, ozone and specific humidity.

Similarly, the changes in the LTE shortwave radiation flux can be written as the sum of the change in shortwave radiation flux due to the direct forcing of CO_2 and the different feedbacks:

$$\Delta\vec{S}_{LTE} = \Delta\vec{S}_{CO_2} + \Delta\vec{S}_{O_3} + \Delta\vec{S}_{H_2O} + \Delta\vec{S}_{albedo} + \Delta\vec{S}_{cloud} \qquad (10)$$

Similarly, to equation (9), we perform a linearization.

Substituting (9) and (10) in equation (8) yields:

$$\Delta(\vec{S}-\vec{R})_{CO_2} + \Delta(\vec{S}-\vec{R})_{O_3} + \Delta(\vec{S}-\vec{R})_{H_2O} + \Delta(\vec{S}-\vec{R})_{albedo} + \Delta(\vec{S}-\vec{R})_{cloud} - \frac{\partial\vec{R}}{\partial\vec{T}}\Delta T$$
$$+\Delta(\vec{S}-\vec{R})_{non-LTE} + \Delta dyn = 0 \quad (11)$$

This can be written as:

$$\frac{\partial\vec{R}}{\partial\vec{T}}\Delta T = +\Delta(\vec{S}-\vec{R})_{non-LTE} + \Delta dyn \quad (12)$$

Equation (12) can be solved for the individual temperature perturbations. We calculate the temperature changes due to the direct effect of CO_2 as well as the different feedback processes.

$$\Delta T_{CO_2} = \left(\frac{\partial\vec{R}}{\partial\vec{T}}\right)^{-1} \Delta(\vec{S}-\vec{R})_{CO_2} \quad (13)$$

This can be done in a similar way for the different feedback processes:

$$\Delta T_{O_3} = \left(\frac{\partial\vec{R}}{\partial\vec{T}}\right)^{-1} \Delta(\vec{S}-\vec{R})_{O_3} \quad (14)$$

$$\Delta T_{H_2O} = \left(\frac{\partial\vec{R}}{\partial\vec{T}}\right)^{-1} \Delta(\vec{S}-\vec{R})_{H_2O} \quad (15)$$

$$\Delta T_{albedo} = \left(\frac{\partial\vec{R}}{\partial\vec{T}}\right)^{-1} \Delta(\vec{S}-\vec{R})_{albedo} \quad (16)$$

$$\Delta T_{cloud} = \left(\frac{\partial\vec{R}}{\partial\vec{T}}\right)^{-1} \Delta(\vec{S}-\vec{R})_{cloud} \quad (17)$$

The factors $\Delta(\vec{S}-\vec{R})_{CO_2}$, $\Delta(\vec{S}-\vec{R})_{O_3}$, $\Delta(\vec{S}-\vec{R})_{H_2O}$, $\Delta(\vec{S}-\vec{R})_{albedo}$ and $\Delta(\vec{S}-\vec{R})_{cloud}$ are calculated by inserting the output variables from WACCM in the radiation code of CFRAM. Here, one takes the output variables from the control run, apart from the variable that is related to the direct forcing or the feedback.

This means that for the direct forcing of CO_2, one takes the CO_2 from the perturbation run, while one takes the other variables from the control run. For the ozone feedback, one takes the ozone from the perturbation run. For the water vapour feedback, one takes the specific humidity, surface pressure, surface temperature and dew point temperature. While for the albedo feedback, one takes the downwelling solar flux at surface and net solar flux at surface from the perturbation run and the other variables from the control run.

For the cloud feedback, one takes the cloud fraction, cloud ice and cloud liquid amount from the perturbation run. For all these feedbacks, one takes the other variables from the control run.

Similarly to equations (13)-(17), we also calculate the temperature change due to non-LTE processes and the dynamical feedback. We already calculated the terms $\Delta(\vec{S}-\vec{R})_{non-LTE}$ and Δdyn in (4) and (7).

$$\Delta T_{non-LTE} = \left(\frac{\partial\vec{R}}{\partial\vec{T}}\right)^{-1} \Delta(\vec{S}-\vec{R})_{non-LTE} \quad (18)$$

$$\Delta T_{dyn} = \left(\frac{\partial\vec{R}}{\partial\vec{T}}\right)^{-1} \Delta dyn \quad (19)$$

The calculated partial temperature changes can be added, their sum being equal to the total temperature change. It is important to note that this does not mean that the individual processes are physically independent of each other.

$$\Delta T_{CFRAM} = +\Delta T_{O_3} + \Delta T_{H_2O} + \Delta T_{albedo} + \Delta T_{cloud} + \Delta T_{non-LTE} + \Delta T_{dyn} \quad (20)$$

The linearization done for equations (9) and (10) introduces an error between the temperature difference as calculated by CFRAM and as seen in the model output. Another source of error is that the radiation code of the CFRAM calculations is not exactly equal to the radiation code of WACCM.

$$\Delta T_{CFRAM} = \Delta T_{WACCM} - \Delta T_{error} \quad (21)$$

For more details on the CFRAM method, please refer to *Lu and Cai* (2009).

Note that the method used in this study differs from the Middle Atmosphere Climate Feedback Response Analysis Method (MCFRAM) used by *Zhu et al.* (2016). The major difference is that in this study, we perform the calculations using the units of energy fluxes (Wm^{-2}) instead of converting to heating rates (Ks^{-1}). Another difference is that our method is not applicable above 0.01 hPa (~80 km), while *Zhu et al.* (2016) added molecular thermal conduction to the energy equation, to perform the calculations beyond the mesopause.

3. Results

3.1 Temperature responses in a double CO_2 scenario

In section 2.2, it was discussed that four experiments were performed with WACCM: a simulation with pre-industrial conditions, a simulation with changed SSTs only, a simulation with only a changed CO_2-concentration and a final simulation with both changed SSTs and CO_2-concentration.

Figure 1 shows the zonal mean temperature changes for the different experiments with respect to the pre-industrial state, as modelled by WACCM. As shown in earlier studies, we observe that an increase in CO_2 causes a cooling in the middle atmosphere with the exception of the cold summer upper mesosphere region (*Akmaev*, 2006). We also observe that changing the SSTs alone, while leaving the CO_2-concentration at the pre-industrial levels (Fig 1c and 1f) also yields significant temperature changes over a large part of the middle atmosphere, and contributes to the observed warming in the cold summer mesopause region.

In line with *Fomichev et al.* (2007) and *Schmidt et al.* (2006), we find that the sum of the two separate temperature changes in the experiment with changed CO_2 only and changed SSTs only is approximately equal to the changes observed in the combined simulation. *Shepherd* (2008) has explained this phenomenon as follows: climate change affects the middle atmosphere in two ways: either radiatively through in situ changes associated with changes in CO_2 or dynamically through changes in stratospheric wave forcing, which are primarily a result of changing the SSTs (*Shepherd,* 2008). Even though the radiative and dynamic processes are not independent, at first approximation, these processes are seen to be additive (*Sigmond et al.*, 2004, *Schmidt et al.,* 2006, *Fomichev et al.,* 2007).

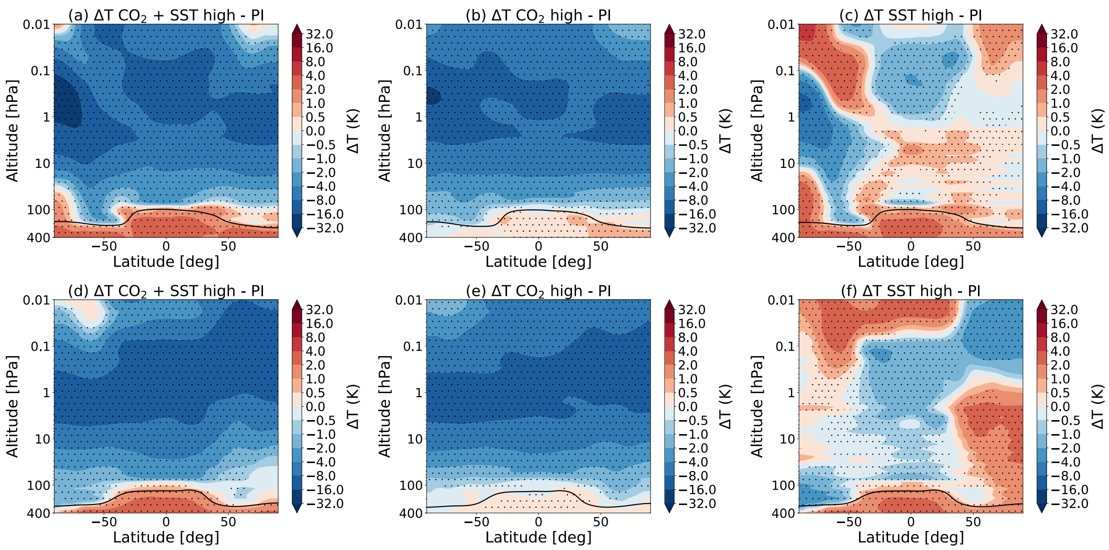

Figure 1: The total change in temperature in July (top) and January (bottom) for (a,d) the simulation with high CO_2 and SSTs, (b,e) the simulation with high CO_2, (c,f) the simulation with high SSTs, all as compared the pre-industrial control simulation. The dotted regions indicate the regions where the data reaches a confidence level of 95%. The black line indicates the tropopause height for the runs with changed CO_2-concentration and SSTs (a,d), with changed CO_2-concentration (b,e) and with changed SSTs (c,f).

The CFRAM makes it possible to separate and estimate the temperature responses due to an external forcing and various climate feedbacks, such as ozone, water vapour, cloud, albedo and dynamical feedbacks. Note that for the ozone, water vapour, cloud and albedo feedback, we can only calculate the radiative part of the feedback.

Because we are using an atmosphere-only model, in our experiment, the external forcing is either the change in CO_2-concentration or the change in SSTs or both. In an atmosphere-ocean model (such as CESM) and, of course, in reality the changes in sea surface temperature and sea ice distributions are responses to the changed CO_2-concentration.

Figure 2 shows the average change in global mean temperature for the lower stratosphere, the upper stratosphere and the mesosphere for the experiment with the changed CO_2-concentration and changed SSTs. To calculate the lower stratosphere temperature changes, we take the average value of the temperature change from the tropopause – the pressure level of which is an output of WACCM – until about 24 hPa for each latitude.

The tropopause is not exactly at the same pressure level, we always take the one for the perturbation experiment which is a bit higher at some latitudes, to make sure that we don't use values from the troposphere. We add the values for each latitude up and take the average. This average is not mass weighted. The temperature changes in the upper stratosphere and in the mesosphere are calculated in the same way, but then for the altitudes 24 hPa-1 hPa and 1 hPa-0.01 hPa respectively.

Figure 2 shows the radiative feedbacks due to ozone, water vapour, clouds, albedo and the dynamical feedback, as well as the small contribution due to the Non-LTE processes, as calculated by CFRAM. The 'total'-column shows the temperature changes in WACCM, while the column 'error' shows the difference between temperature change in WACCM and the sum of the calculated temperature responses in CFRAM. In sections 3.3-3.6, we will discuss the different feedbacks separately in more detail, at this point we give an overview of the general effects and relative importance of the different feedback processes.

Figure 2 shows that the temperature change in the lower stratosphere due to the direct forcing of CO_2 is around 3 K. We also observe that there is a cooling of about 1 K due to ozone feedback in the tropical region while there is a slight warming taking place in the summer hemispheres in both January and July. We also see that the temperature change in the lower stratosphere is influenced by the water vapour feedback and to a lesser degree by the cloud and albedo feedback.

In the upper stratosphere, the cooling due to the direct forcing of CO_2 is with about 9 degrees considerably stronger than in the lower stratosphere. The water vapour, cloud and albedo feedback play no role in the upper stratosphere and mesosphere. The ozone feedback results in the positive partial temperature changes, of about 2 K. The picture in the mesosphere is similar. The main difference is that the temperature changes are larger, note the difference of the range for the temperature change between Fig. 2c, d and Fig. 2e,f.

The ozone feedback generally yields a radiative feedback that mitigates the cooling, which is due to the direct forcing of CO_2. This has been suggested in earlier studies, such as *Jonsson et al., 2004*. With CFRAM, it is possible to quantify this effect and to compare it with the effects of other feedbacks in the middle atmosphere.

The temperature response due to dynamical feedbacks is small in global average. This can be understood as waves generally do not generate momentum and heat, but redistribute these instead (*Zhu et al.,* 2016). However, the local responses to dynamical changes in the high latitudes are large, as we will see in section 3.3. There are some small temperature responses due to non-LTE effects as well.

The error term is relatively large. In CFRAM, we assumed that the radiative perturbations can be linearized by neglecting the higher order terms of each thermodynamic feedback and the interactions between these feedbacks, this yields an error. Cai and Lu (*2009*) show that this error is larger in the middle atmosphere than for similar calculations in the troposphere. In the middle atmosphere, the density of the atmosphere is smaller, which leads to smaller numerical values of the diagonal elements of the Planck feedback matrix. As a result, the linear solution is very sensitive to forcing in the middle atmosphere. Another part of the error is due to the fact that the radiative we use in CFRAM is relatively simple, as compared to the one that is used in WACCM.

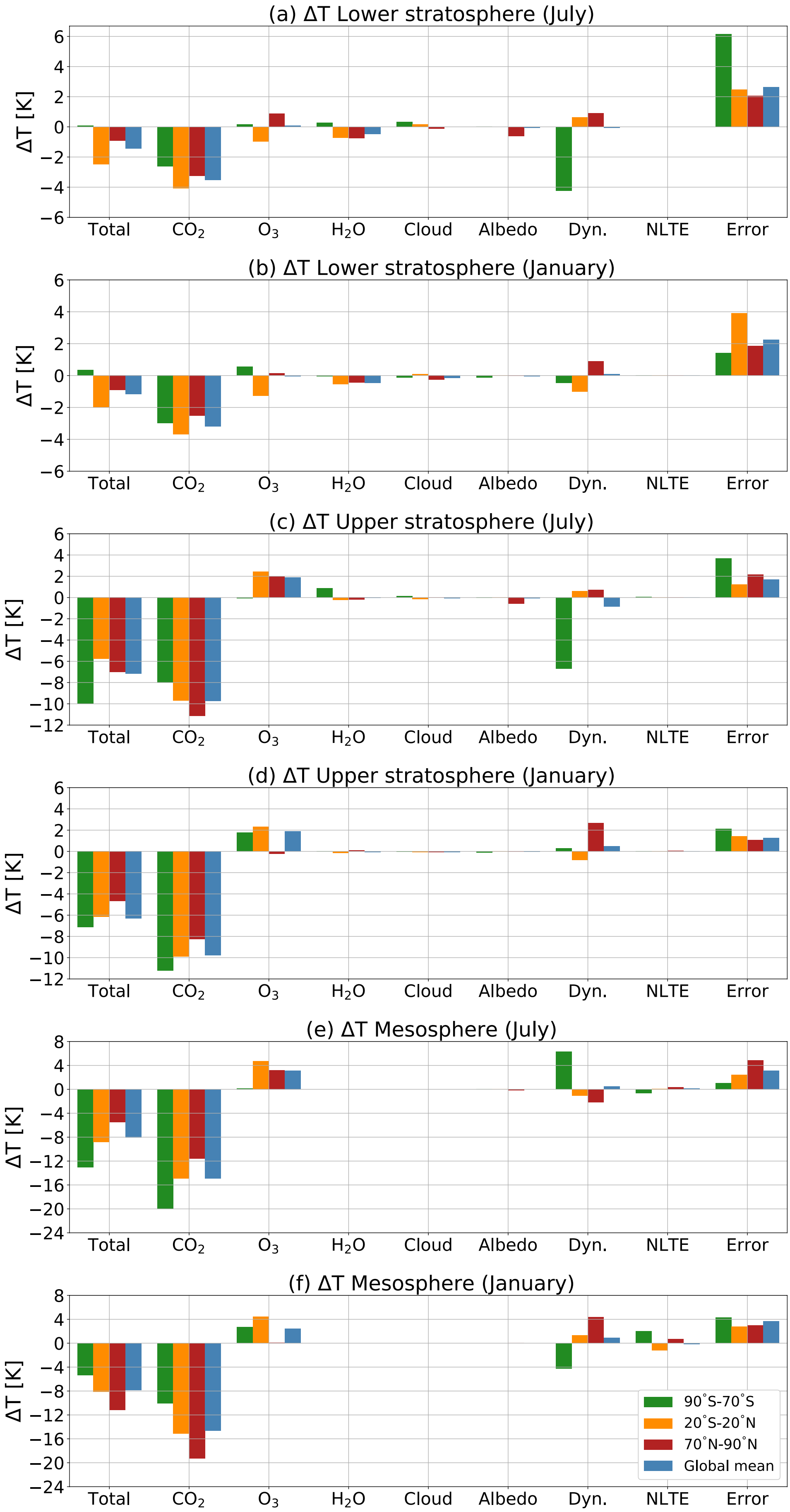
(a) ΔT Lower stratosphere (July)
(b) ΔT Lower stratosphere (January)
(c) ΔT Upper stratosphere (July)
(d) ΔT Upper stratosphere (January)
(e) ΔT Mesosphere (July)
(f) ΔT Mesosphere (January)
ΔT [K]
Total
CO2
O3
H2O
Cloud
Albedo
Dyn.
NLTE
Error
90˚S-70˚S
20˚S-20˚N
70˚N-90˚N
Global mean

Figure 2: The mean temperature responses to the changes in CO_2 and various feedback processes in the lower stratosphere from the tropopause height until 24 hPa (a,b), upper stratosphere from 24-1 hPa (c, d) and in the mesosphere from 1-0.01 hPa (e,f) in July (a, c, e) and January (b, d, f) in the polar regions (90°S-70°S and 70°N-90°N), the tropics (20°S-20°N) and the global mean, for experiment with double CO_2 and changed SSTs.

In addition, the vertical profiles of the temperature responses to the direct forcing of CO_2 and the feedbacks are shown in Figure 3. Here, one can see that the increase in CO_2 leads to a cooling over almost the whole middle atmosphere; an effect that increases with height. We also observe that in the summer upper mesosphere regions, the increased CO_2-concentration leads to a warming. The changes in ozone concentration in response to the doubling of CO_2 leads to warming almost everywhere in the atmosphere. In some places, this warming exceeds 5 K. In the polar winter the effect of ozone is small due to lack of sunlight.

There is also a relatively large temperature response to the changes in dynamics. In Fig. 3, it can be seen that there is a cooling in the summer mesosphere, while there is warming in the winter mesosphere. The water vapour, cloud and albedo feedback play only a very small role in the middle atmosphere, as we observed in Figure 2. The Non-LTE effects are also small, but start to play a small role above 0.1 hPa, the exact mechanism of which is outside the scope of this paper.

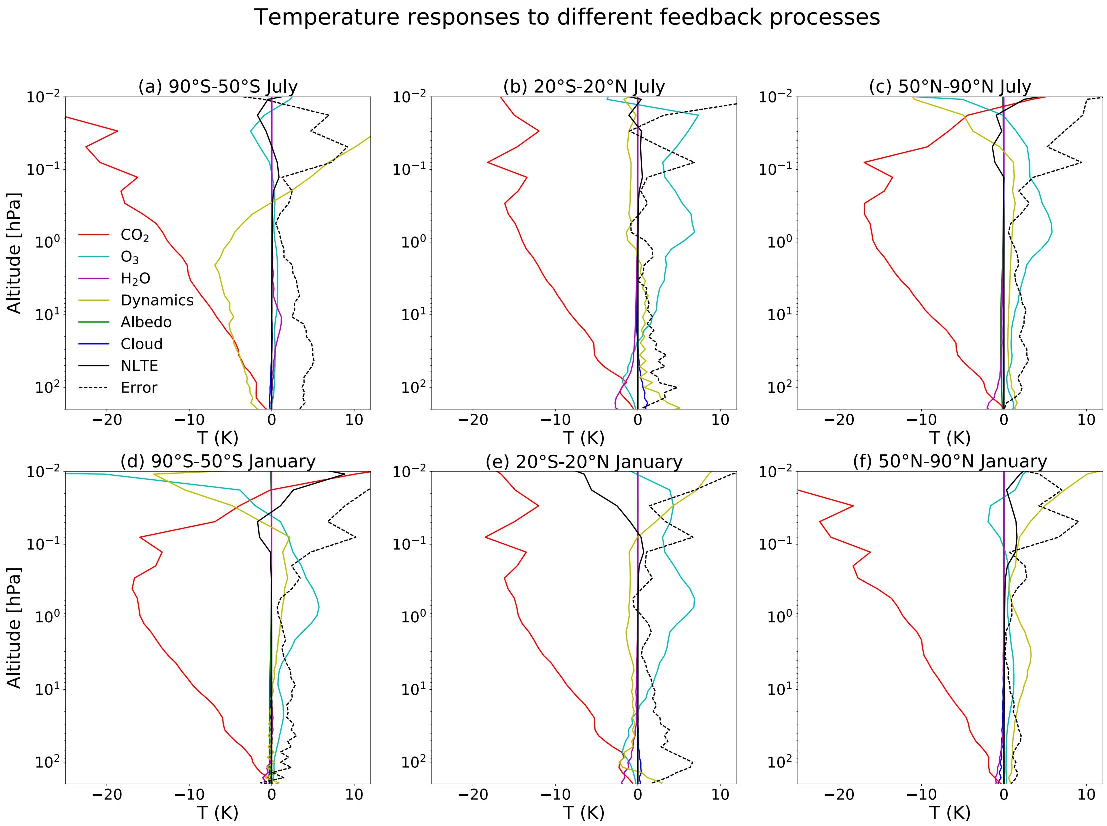

Figure 3: Vertical profiles of the temperature responses to the changes in CO_2 and various feedback processes in July (top) and January (bottom) for the experiment with double CO_2 and changed SSTs in the atmosphere between

200 and 0.01 hPa, for regions from 50° N/S polewards and the tropics (20°S-20°N), as calculated by CFRAM.

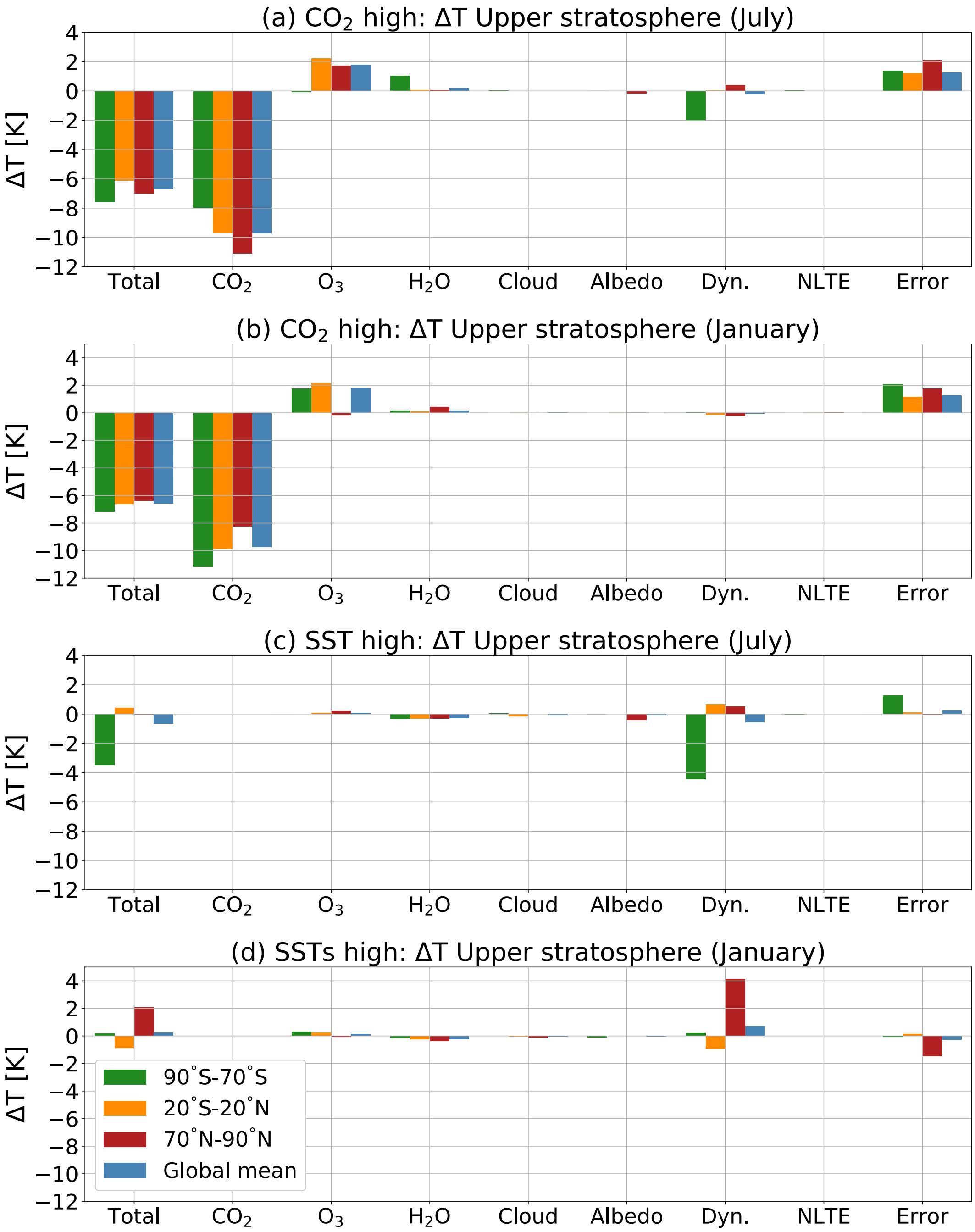

Figure 4: The mean temperature responses to the changes in CO_2 and various feedback processes in July (a,c) and January (b,d) in the upper stratosphere between 24 and 1 hPa, for polar regions (90°S-70°S and 70°N-90°N), the tropics (20°S-20°N) and the global mean for the experiment with double CO_2 (a,b) and changed SSTs (c,d) separately.

Figure 4 shows temperature responses in the upper stratosphere for the experiment with double CO_2 (a,b) and changed SSTs (c,d) separately. These temperature changes were calculated as they were for Fig. 2. Again also, the 'total'-column shows the temperature changes as found by WACCM, the columns CO_2, O_3, H_2O, cloud, albedo, dynamics, Non-LTE shows the temperature responses as calculated by CFRAM. Error shows the difference between temperature change in WACCM and the sum of the calculated temperature responses in CFRAM.

We learn from this figure that the effects of the changed SSTs on the middle atmosphere are relatively small as compared to the effects of changing the CO_2. The changes in SSTs are responsible for large temperature changes as a result of the dynamical feedbacks, especially in the winter hemispheres. A similar figure for the lower stratosphere (not shown) shows that the the temperature response to the water vapour feedback is, however, almost solely due to changes in the SSTs.

Earlier, we discussed that the sum of the two separate temperature changes in the experiment with double CO_2 and changed SSTs is approximately equal to the changes observed in the combined simulation. We find that the same is true for the temperature responses to the different feedback processes.

In the rest of the paper, we discuss the temperature responses to the direct forcing and the various feedbacks during July and January in further detail.

3.2 Temperature direct response to CO_2

Figure 5 shows the zonal mean temperature change due to the increase in CO_2. We see that increasing CO_2 leads to a cooling almost everywhere in the middle atmosphere, except at the high latitudes in the cold summer upper mesosphere. The higher the temperature, the more cooling there is taking place due to the increasing CO_2-concentration (*Shepherd,* 2008). The reason for this is that the outgoing longwave radiation strongly depends on the Planck blackbody emission (*Zhu et al.,* 2016).

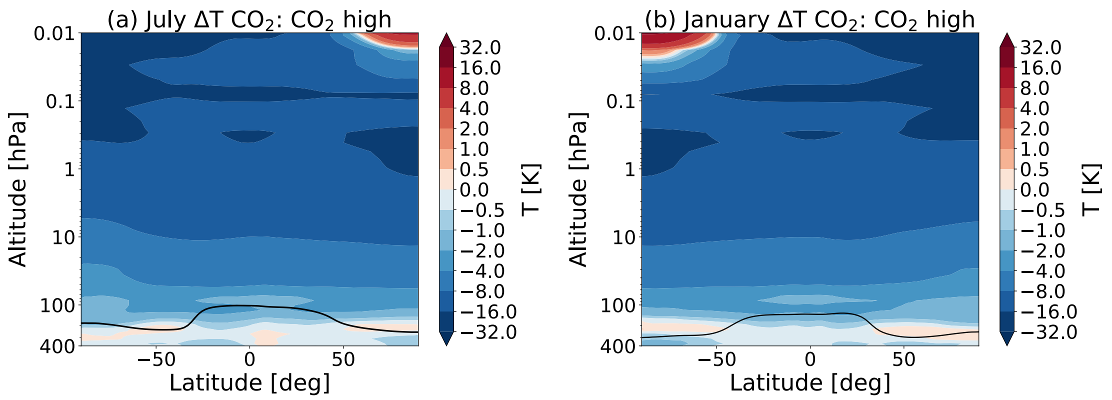

Figure 5: Temperature changes to direct CO_2 forcing in July (left) and January (right) for the high CO_2 simulation as compared to pre-industrial control simulation, as calculated by CFRAM. The black line indicates the tropopause height for the runs with changed CO_2-concentration.

Changing the SSTs does not lead to a change in CO_2-concentration, therefore the temperature response to changes in CO_2 is not present for the run with only changed SST (Figures not shown).

3.3 Dynamical feedback

Ozone is the largest feedback, which mitigates the cooling due to the direct CO_2 forcing in most parts of the middle atmosphere (Fig. 2). Climate change affects stratospheric ozone through changes in middle atmospheric chemistry, through changes in dynamics or a combination of these two factors. To understand how the ozone concentration is changing, it is necessary to understand how the dynamics in the middle atmosphere is altered in a double CO_2 climate. Therefore, we will first go into the dynamics of the middle atmosphere and the temperature responses to dynamical changes.

As discussed in the introduction, in the middle atmosphere there is a wave driven circulation which drives the temperatures away from radiative equilibrium. Large departures from this radiative equilibrium state are seen in the mesosphere and in the polar winter stratosphere. In the mesosphere, there is a zonal forcing, which yields a summer to winter transport. In the polar winter stratosphere, there is a strong forcing that consists of rising motion in the tropics, poleward flow in the stratosphere and sinking motion in the middle and high latitudes. This circulation is referred to as the 'Brewer-Dobson circulation' (*Butchart et al*. 2010).

The zonal mean residual circulation forms an important component of the mass transport by the BDC. It consists of a merional ($\bar{v}^*$) and a vertical ($\bar{w}^*$) component as defined in the Transformed Eulerian Mean (TEM) framework. The residual circulation consists of a shallow branch which controls the transport of air in the tropical lower stratosphere, as well as a deep branch in the mid-latitude upper stratosphere and mesosphere.

Both of these branches are driven by atmospheric waves. In the winter hemisphere, planetary Rossby waves propagate upwards into the stratosphere, where they break and deposit their momentum on the zonal mean flow, which in turns induces a meridional circulation. The two-cell structure in the lower stratosphere, which is present all-year round, is driven by synoptic waves. The circulation is also affected by orographic gravity wave drag in the stratosphere and by non-orographic gravity wave drag in the upper mesosphere (*Oberländer et al*., 2013).

Most climate models show that the BDC and the upwelling in the equatorial region will speed up due to an increase in CO_2-concentration (*Butchart el al.,* 2010). It has been shown that the strengthening of the Brewer-Dobson circulation in the lower stratosphere is caused by changes in transient planetary and synoptic waves, while the upper stratospheric changes are due to changes in the propagation properties for gravity waves (*Oberländer et al*., 2013).

It has been explained that the increased stratospheric resolved wave drag is caused by an increase of the meridional temperature gradient in the stratosphere, which leads to a strengtening of the upper flank of the subtropical jets. This in turn shifts the critical layers for Rossby wave breaking upward, which allows for more Rossby waves to reach the lower stratosphere, where they break and deposit their momentum, enhancing the BDC (*Shepherd and McLandress*, 2011)

The differences in the meridional component of the residual circulation ($\bar{v}^*$) between the different simulations are shown in Fig. 6. These data are averaged over the 40 years of data. Figure 6b and 6e show that only doubling the CO_2 leads to a stronger pole-to-pole flow in the mesosphere. Changing the SSTs also leads to changes in the residual circulation as can be seen in Fig. 6c and 6f. Oberländer et al. (*2013*) have shown that the rising CO_2-concentration affects the upper stratospheric layers, while the signals in the lower stratosphere are almost completely due to changes in sea surface temperature.

The warmer sea surface temperatures enhance the activity of transient planetary waves and orographic gravity waves in the lower and middle stratosphere, for example via the amplification of deep convection (*Deckert and Damaris, 2008*). The changed SSTs also leads to enhanced dissipation of planetary waves, as well as orographic and non-orographic waves in the upper stratosphere.

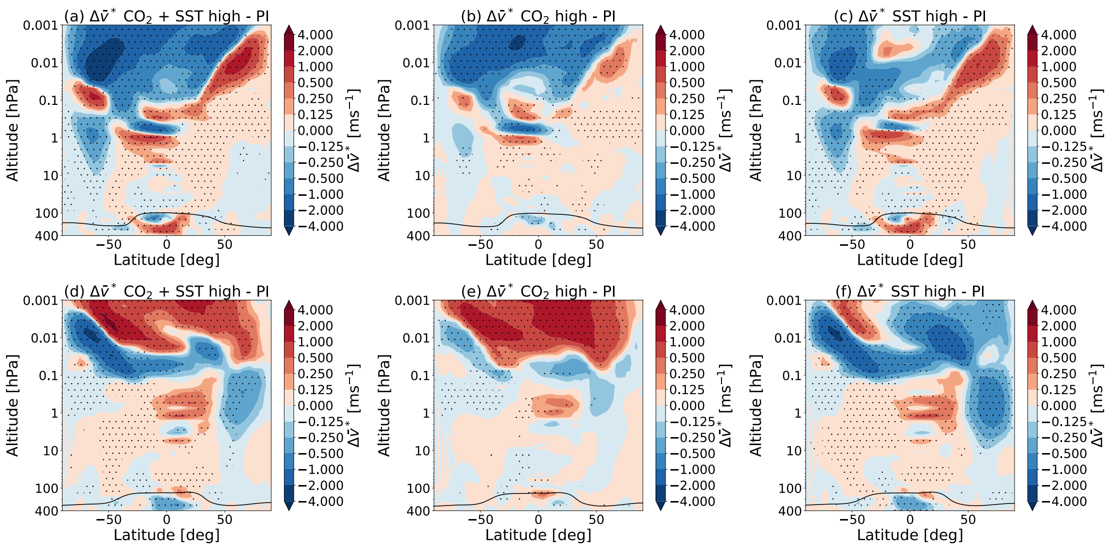

Figure 6: The changes in transformed Eulerian-mean residual circulation horizontal velocity $\bar{v}^*$ in July (top) and January (bottom) for (a,d) the simulation with high CO_2 and SSTs, (b,e) the simulation with high CO_2, (c,f) the simulation with high SSTs, all as compared to pre-industrial control simulation, as found by WACCM. The dotted regions indicate the regions where the data reaches a confidence level of 95%. The black line indicates the tropopause height for the runs with changed CO_2-concentration and SSTs (a,d), with changed CO_2-concentration (b,e) and with changed SSTs (c,f).

We are interested in the temperature responses due to the dynamical feedbacks in the different experiments. These temperature responses are shown in Figure 7. Figure 7b and 7e show that there is cooling in the summer mesosphere, while there is warming in the winter mesosphere, which is consistent with a stronger summer-to-winter pole flow.

Figure 7c and 7f show the temperature responses due to changes in the SSTs. It is seen that there is mostly a warming in the summer mesosphere and mostly a cooling in the winter hemisphere, which would weaken the effect of the changed CO_2-concentration. Most of the temperature responses in the lower stratosphere are caused by the changes in SSTs, as expected.

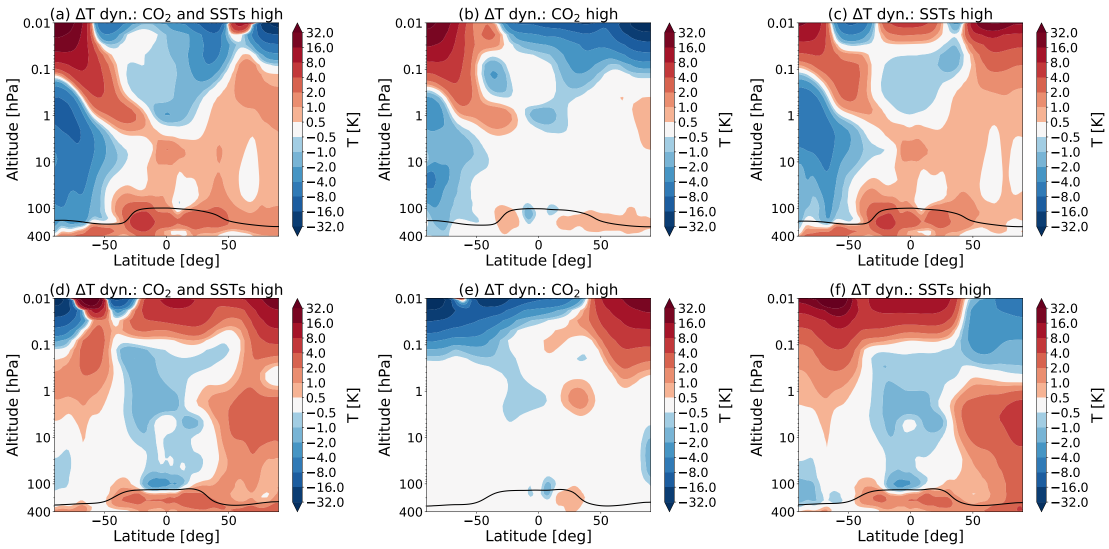

Figure 7: Temperature responses to changes in dynamics, as calculated by CFRAM, in July (top) and January (bottom) for (a,d) the simulation with high CO2 and SSTs, (b,e) the simulation with high CO2, (c,f) the simulation with high SSTs, all as compared to pre-industrial control simulation. The tropopause height is indicated as in Fig. 6.

In summary, doubling the CO_2 leads to a stronger pole-to-pole flow in the mesosphere, which leads to cooling of the summer mesosphere and a warming of the winter mesosphere. Changing the SSTs weakens this effect, but leads to temperature changes in the stratosphere and lower mesosphere.

3.4 Ozone feedback

Ozone plays a major role in the chemical and radiative budget of the middle atmosphere. The ozone distribution in the mesosphere is maintained by a balance between transport processes and various catalytic cycles involving nitrogen oxides, HO_x and Cl_x radicals. In the upper stratosphere, NO_x and Cl_x cycles dominate (*Cariolle*, *1982*), while OH is of utmost importance in the mesosphere (*Jonsson et al., 2004*).

In this paper, we are interested in the changes in ozone concentration induced by the increased CO_2 concentration and/or the changes in SST in

WACCM. In the real world, the ozone concentration is not only affected by the changing CO_2 concentration, but also by CFC and NO_x emissions.

Fig. 8 shows the percentage changes in O_3-concentration when the CO_2-concentration and/or the SSTs change. An increase in CO_2, leads to an increase of ozone in most of the middle atmosphere. However, in the tropical lower stratosphere, the summer polar mesosphere, the winter and equatorial mesosphere, a decrease in ozone is seen. Fig. 8c and f show that changing the SSTs also has a significant impact on the ozone concentration. A complete account of the ozone changes is out of the scope of this paper, but the main processes responsible for ozone changes will be discussed.

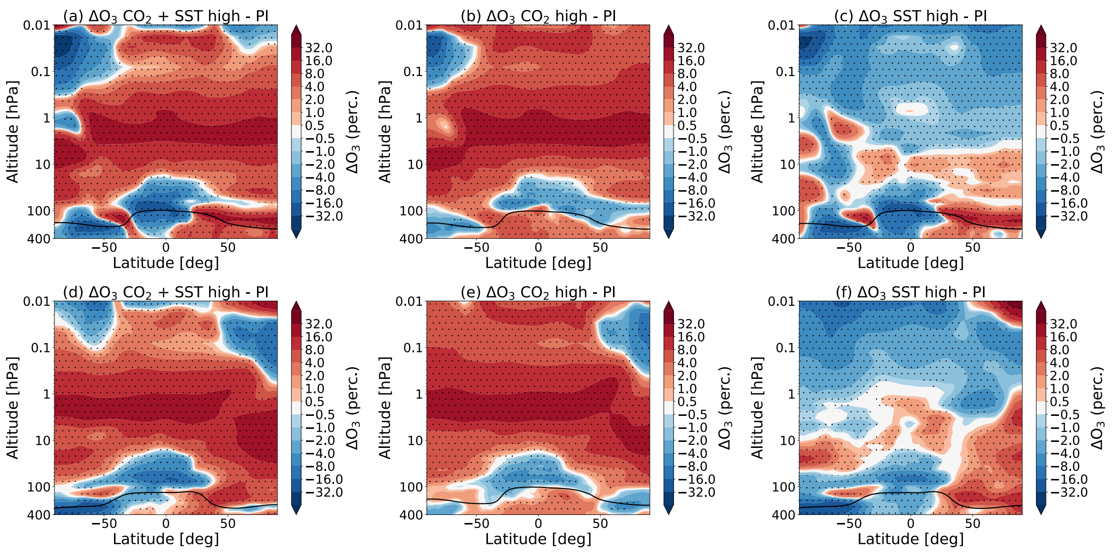

Figure 8: The percentage changes in ozone concentration in July (top) and January (bottom) for (a,d) the simulation with high CO2 and SSTs, (b,e) the simulation with high CO2, (c,f) the simulation with high SSTs, all as compared to the pre-industrial control simulation, as found by WACCM. The statistical signifance and tropopause height are indicated as in Fig. 6.

Ozone chemistry is complex, however the ozone increase between 30 - 70 km can be understood primarily as a result of the negative temperature dependence of the reaction $O + O_2 + M \rightarrow O_3 + M$. The fractional contribution of this processes and other loss cycles involving NO_x, CLO_x and NO_x varies with altitude.

At altitudes between 50 and 60 km, the ozone increase is understood by less effective HO_X odd oxygen destruction. The increase in O_3 between 45 and 50 km can be understood as the reaction rate coefficient of the sink reaction $O + O_3 \rightarrow 2O_2$ decreases. At altitudes lower than 45 km, there is a decrease of NO_x abundance, which can explain the increase (*Jonsson et al.,* 2004).

Schmidt et al. (*2006*) show that the decrease of ozone at the high latitudes in the summer mesosphere, is due to a decrease in atomic oxygen which results from increased upwelling. The decrease in O_3 concentration in the polar winter around 0.1 hPa is due to a stronger subsidence of NO and Cl, which are both ozone-destroying constituents.

The temperature responses due to the ozone feedback are shown in Figure 9. It can be seen that there is a warming in the regions, where there is an increase of the O_3-concentration, while there is a cooling for the regions with a decrease of the O_3-concentration. However, this is not the case for the winter polar region, where there is no sunlight. Note that the temperature responses to the changes in CO_2- and O_3- concentration behave differently in this respect: the temperature responses due to the direct forcing of CO_2 follow the temperature distribution quite closely, while the temperature responses due to O_3 follow the ozone concentration, as also seen by *Zhu et al.,* (2016).

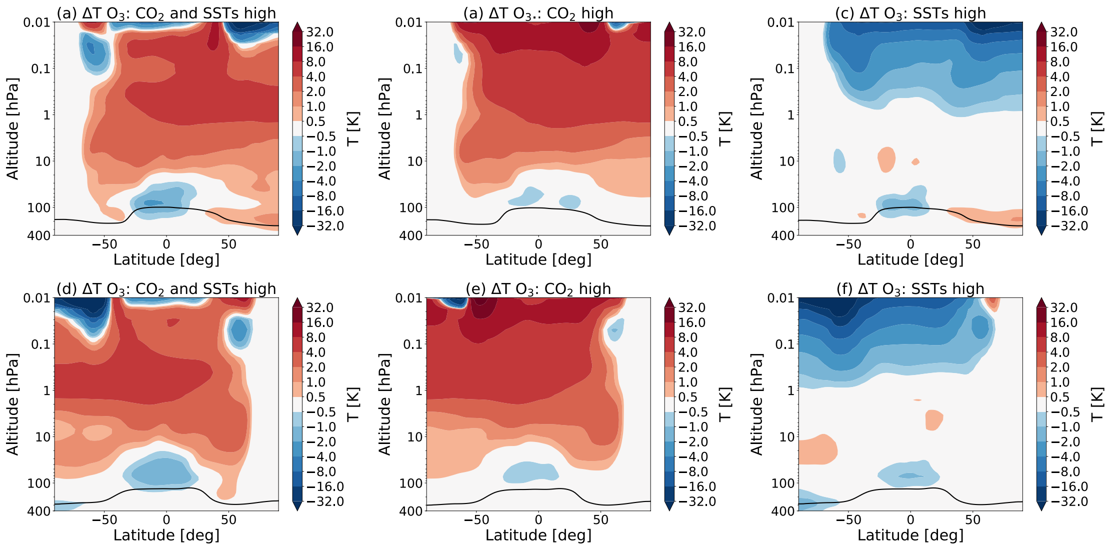

Figure 9: Temperature responses to changes in O_3-concentration, as calculated by CFRAM, in July (top) and January (bottom) for (a,d) the run with high CO2 and SSTs, (b,e) the run with high CO2, (c,f) the run with high SSTs, all as compared to pre-industrial conditions. The tropopause height is indicated as in Fig. 6.

3.5 Water vapour feedback

Water vapour plays a secondary but not negligible role in determining the middle atmosphere climate sensitivity. In Figure 3, we saw the temperature responses to the different feedbacks between 20°S and 20°N in July and January for changes in both the SSTs and the CO_2-concentration. It can be seen that in the lower stratosphere, H_2O contributes considerably to the cooling in this region. Above 30 hPa**,** the water vapour contribution to the energy budget is negligible, as also seen by *Fomichev et al.* (2007).

Figure 10 shows how the water vapour is changing in the middle atmosphere if the CO_2-concentration and/or the SSTs are enhanced. In WACCM, increasing the CO_2-concentration alone leads to a decrease of water vapour in most of the middle atmosphere (Fig. 10 b and f).

The amount of water vapour in the stratosphere is determinged by transport through the tropopause as well as by the oxidation of methane in the stratosphere itself. The transport of the water vapour in the stratosphere is mainly a function of the tropopause temperature (*Solomon et al.,* 2010). In WACCM, we see a decrease in temperature in the tropical tropopause for the double CO_2 experiment in WACCM of about -0.25 K. The cold temperatures in the tropical tropopause lead to a reduction of water vapour of between 2 and 8% due to freeze-drying in this region.

It can be seen that changing the SSTs leads to an increase in water vapour almost everywhere in the middle atmosphere (Fig. 10c and f). In WACCM, the increase in SSTs is observed to lead a higher and warmer tropopause, which can explain this increase of water vapour. However, it should be noted that models currently have a limited representation of the processes determining the distribution and variability of lower stratospheric water vapour. Minimum tropopause temperatures aren't consistently reproduced by climate models (*Solomon et al.,* 2010; *Riese et al.,* 2012). At the same time, observations are not completely clear about whether there is a persistent positive correlation between the SST and the stratospheric water vapour neither (*Solomon et al.*, 2010).

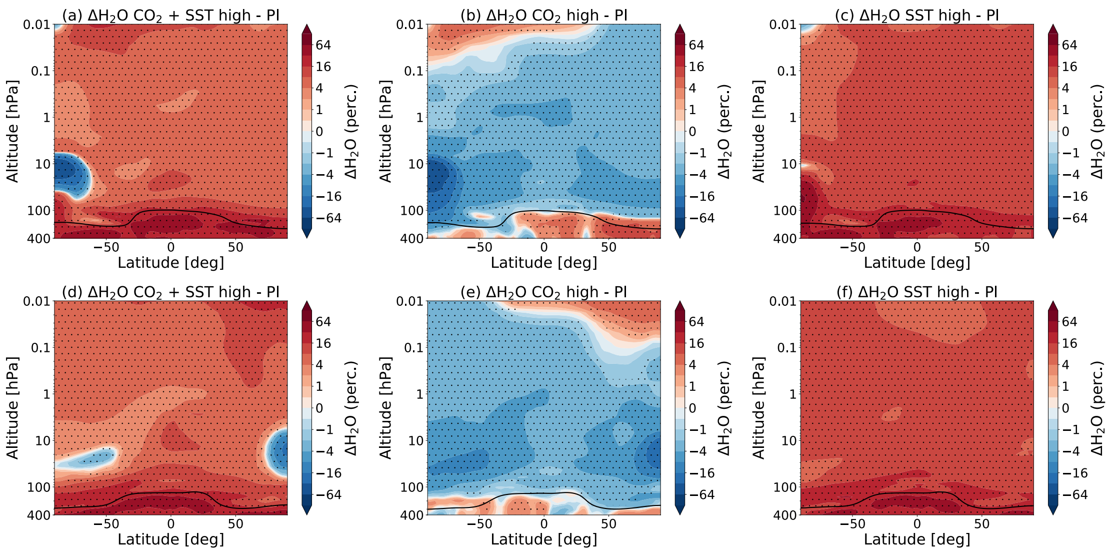

Figure 10: The percentage changes in water vapour mixing ratio in July (top) and January (bottom) for (a,d) the run with high CO2 and SSTs, (b,e) the run with high CO2, (c,f) the run with high SSTs, all as compared to pre-industrial conditions, as found by WACCM. The statistical significance and tropopause height are indicated as in Fig. 6.

Figure 11 shows the temperature responses due to the changes in water vapour as calculated by CFRAM. It can be seen that the regions where there is an increase in the water vapour, there is a cooling, and vice versa. This has been explained as an increase (decrease) in water vapour in the middle atmosphere leads to an increase (decrease) in longwave emissions of water vapour in the mid and far-infrared, which leads to a cooling (warming) (*Brasseur and Solomon,* 2005). Higher up in the atmosphere, there are large percentage changes in water vapour, but the absolute concentration of water is small there, which explains why there is no temperature response to these changes.

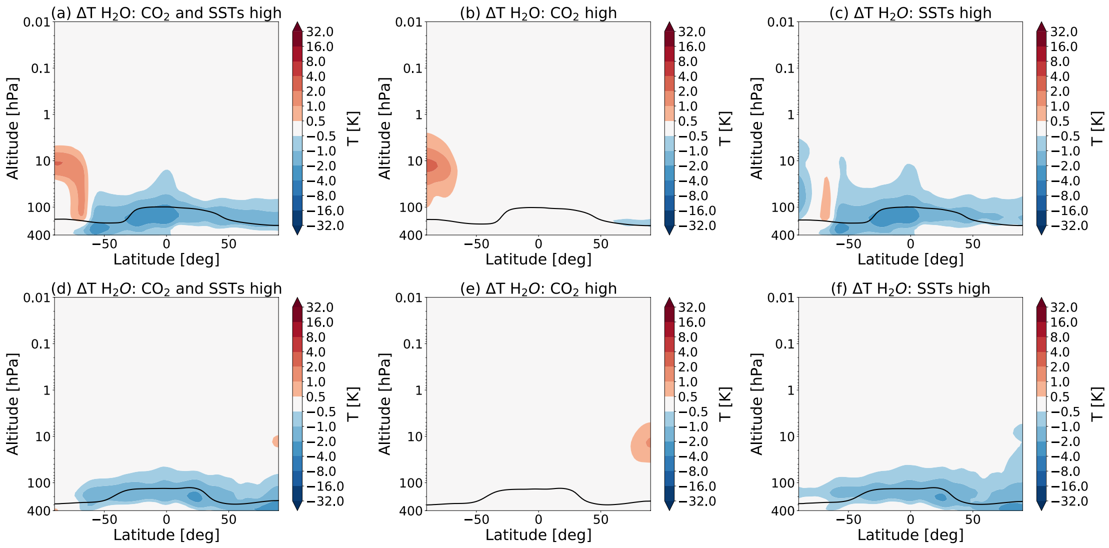

Figure 11: Temperature responses to changes in H_2O-concentration in July (top) and January (bottom) for (a,d) the run with high CO_2 and SSTs, (b,e) the run with high CO2, (c,f) the run with high SSTs, all as compared to pre-industrial conditions, as calculated by CFRAM. The tropopause height is indicated as in Fig. 6.

3.6 Cloud and albedo feedback

It is known that feedbacks due to changes in clouds and surface albedo play a crucial role in determining the tropospheric and surface climate (*Boucher et al.,* 2013, *Royer et al.,* 1990). We have seen in Figure 2 that these feedbacks play only a very small role in the middle atmosphere temperature response to the doubling of CO_2 and SSTs. However, there are some small radiative effects from the cloud and albedo feedback, that are the result of the changes in SSTs, as shown in Figure 12.

Changes in SSTs yield an overall increase in the cloud cover in the upper troposphere, while this is not the case if one only increases the CO_2 concentration. We see that in the tropical region there is a warming due to changes in clouds, while there is a cooling at higher latitudes in July (see Figure 12a). In January, the pattern looks slightly different (see Figure 12c). These temperature changes are due to changes in the balance between the increased reflected shortwave radiation and the decrease of outgoing longwave radiation.

We also see an effect of the changes in surface albedo in the stratosphere (see Figure 12 b and d). The temperature responses shown in Figure 12 b and d are due to radiative changes. The decrease in surface albedo would cause less shortwave radiation being reflected. We suggest that this leads to the cooling seen in the summer polar stratosphere, but more research is needed.

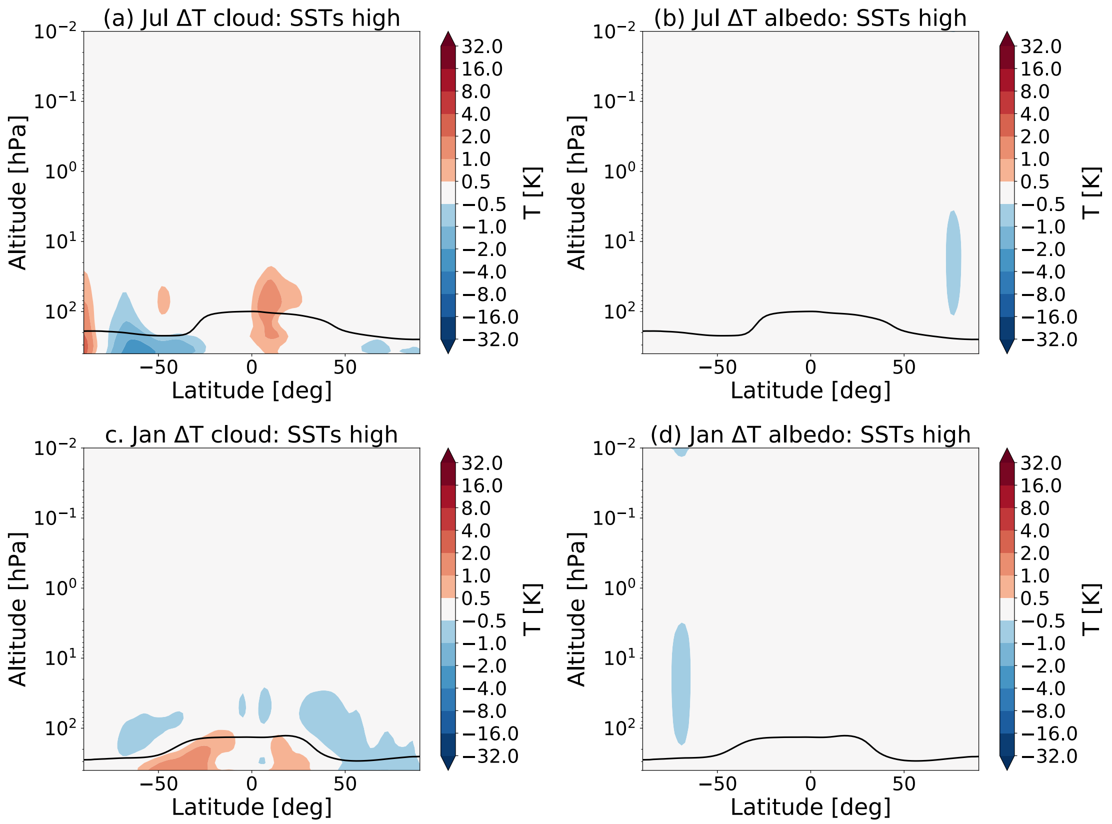

Figure 12: Temperature responses to changes in cloud (left) and albedo (right) in July (top) and January (bottom) for the run with high SSTs as compared to pre-industrial conditions, as calculated by CFRAM. The tropopause height is indicated as in Fig. 6.

4. Discussion and conclusions

In this study, we have applied the climate feedback response analysis method to climate sensitivity experiments performed by WACCM. We have examined the middle atmosphere response to CO_2 doubling with respect to the pre-industrial state. We also investigated the combined effect of doubling CO_2 and subsequent warming SSTs, as well as the effects of separately changing the CO_2 and the SSTs.

It was seen before that the sum of the two separate temperature changes in the experiment with only changed CO_2 and only changed SSTs is, at first approximation, equal to the changes observed in the combined simulation (see e.g. *Fomichev et al. (2007) and Schmidt et al. (2006)*). This is also the case for WACCM.

We have found that, even though changing the SSTs yields significant temperature changes over a large part of the middle atmosphere, the effects of the changed SSTs on the middle atmosphere are relatively small as compared to the effects of changing the CO_2 without changes in the SSTs.

We find that the temperature change due to the direct forcing of CO_2 increases with increasing height in the middle atmosphere. The temperature change in the lower stratosphere due to the direct forcing of CO_2 is around 3 K while in the upper stratosphere, the cooling due to the direct forcing of CO_2 is with about 9 K considerably stronger than in the lower stratosphere. In the mesosphere, the cooling due to the direct forcing of CO_2 is even stronger.

Ozone responds to changes in respond to changes in CO_2 and/or SSTs due to changes in chemical reaction rate constants and due to the strength of the up- and downwelling. The temperature changes caused by these changes in ozone concentration generally mitigate the *cooling* caused by the direct forcing of CO_2. However, we have also seen in that in the tropical lower stratosphere and in some regions of the mesosphere, the ozone feedback cools these regions further.

We also have seen that the global mean temperature response due to dynamical feedbacks is small, while the local responses to the changes in dynamics are large. Doubling the CO_2 leads to a stronger summer-to-winter-pole flow, which leads to cooling of the summer mesosphere and a warming of the winter mesosphere. Changing the SSTs weakens this effect in the mesosphere, but leads to temperature changes in the stratosphere and lower mesosphere.

The temperature change in the lower stratosphere is influenced by the water vapour feedback and to a lesser degree by the cloud and albedo feedback, while these feedbacks play no role in the upper stratosphere and the mesosphere.

It would also be interesting to investigate the exact mechanisms behind the feedback processes in more detail. Some processes can influence the different feedback processes, such as ozone depleting chemicals influencing the ozone concentration and thereby the temperature response of this feedback. Other studies have shown that a surface albedo change, which is associated with sea ice loss, can influence the middle atmosphere dynamics, which in turn influences the temperature response (*Jaiser et al.,* 2013). The CFRAM cannot unravel the effects of these different processes.

There is also a need for a better understanding of how different feedbacks in the middle atmosphere affect the surface climate. As discussed in the introduction, the exact importance of ozone feedback is currently not clear While this paper focused on the temperature changes in the middle atmosphere, similar analysis can be done to quantify the effects of feedbacks on the surface climate.

In conclusion, we have seen that CFRAM is an efficient method to quantify climate feedbacks in the middle atmosphere, although there is a relatively large error due to the linearization in the model. The CFRAM allows for separating and estimating the temperature responses due an external forcing and various climate feedbacks, such as ozone, water vapour, cloud, albedo and dynamical feedbacks. More research into the exact mechanisms of these feedbacks could help us to understand the temperature response of the middle atmosphere and their effects on the surface and tropospheric climate better.

Acknowledgements

The computations and simulations were performed on resources provided by the Swedish National Infrastructure for Computing (SNIC) at National Supercomputer Center (NSC) in Linköping.

Hamish Struthers NSC is acknowledged for assistance concerning technical aspects in making the WACCM code run on NSC supercomputer Tetralith. We thank Qiang Zhang for helping to make the radiation model code applicable to WACCM model data.

Competing interests

The authors have no competing interests to declare.

References

Akmaev, R.A., Fomichev, V.I. and Zhu, X.: Impact of middle-atmospheric composition changes on greenhouse cooling in the upper atmosphere, J. Atmos. Sol. Terr. Phys., 68, 1879-1889, doi:10.1016/j.jastp.2006.03.008, 2006.

Bony, S., and co-authors: How well do we understand and evaluate climate change feedback processes?, Journal of Climate, 19(15), 3445–3482, doi:10.1175/JCLI3819.1, 2006.

Boucher, O., Randall, D., and co-authors: Clouds and Aerosols, in: Climate Change: The Physical Science Basis. Contribution of Working Group I to IPCC AR5, edited by: Stocker T.F. and coauthors., Cambridge University Press, Cambridge, United Kingdom and New York, NY, USA, 2013.

Brasseur, G. P., and Solomon, S.: Aeronomy of the middle atmosphere, Chemistry and physics of the stratosphere, Springer, New York, 2005.

Brewer, A. W. (1949). Evidence for a world circulation provided by the measurements of helium and water vapour distribution in the stratosphere. *Quarterly Journal of the Royal Meteorological Society*, *75*(326), 351-363.

Brühl, C., & Crutzen, P. J.: Scenarios of possible changes in atmospheric temperatures and ozone concentrations due to man's activities, estimated with a one-dimensional coupled photochemical climate model. *Climate Dynamics*, *2*(3), 173-203 (1988).

Butchart, N., and co-authors: Chemistry–climate model simulations of twenty-first century stratospheric climate and circulation changes. J. Climate, 23(20), 5349–5374, doi:10.1175/2010JCLI3404.1, 2010.

Caldwell, P.M., Zelinka, M.D., Taylor, K.E., Marvel, K., 2016: Quantifying the sources of intermodal spread in equilibrium climate sensitivity, J. Clim. 29, 513-524.

Cai, M., and Lu, J.: A new framework for isolating individual feedback processes in coupled general circulation climate models. Part II: Method demonstrations and comparisons, Climate dynamics, 32(6), 887-900, doi:10.1007/s00382-008-0424-4, 2009.

Cariolle, D. (1983). The ozone budget in the stratosphere: Results of a one-dimensional photochemical model. *Planetary and Space Science*, *31*(9), 1033-1052.

Deckert, R., & Dameris, M. (2008). Higher tropical SSTs strengthen the tropical upwelling via deep convection. *Geophysical research letters*, *35*(10).

Dietmüller, S., Ponater, M., and Sausen, R.: Interactive ozone induces a negative feedback in CO2-driven climate change simulations. Journal of Geophysical Research: Atmospheres, 119(4), 1796-1805, 2014.

Dobson, G. M. B. (1956). Origin and distribution of the polyatomic molecules in the atmosphere. *Proceedings of the Royal Society of London. Series A. Mathematical and Physical Sciences*, *236*(1205), 187-193.

Fomichev, V.I., Jonsson, A.I., De Grandpre, J., Beagley, S.R., McLandress, C., Semeniuk, K., Shepherd, T.G.: Response of the middle atmosphere to CO_2 doubling: Results from the Canadian Middle Atmosphere Model, Journal of Climate, 20(7), doi:10.1175/JCLI4030.1, 2007.

Hu, X., Y. Li, S. Yang, Y. Deng and Cai. M.: Process-based decomposition of the decadal climate difference between 2002-13 and 1984-95, J. Climate, 30, 4373–4393, doi: 10.1175/JCLI-D-15-0742.1, 2017.

Hurrell, J., et al.: The Community Earth System Model: A framework for collaborative research, Bull. Am. Meteorol. Soc., doi:10.1175/BAMS-D-12-00121.1, 2013.

Jaiser, R., K. Dethloff and D. Handorf: Stratospheric response to Arctic sea ice retreat and associated planetary wave propagation changes. Tellus A: Dynamic Meteorology and Oceanography, 65(1), 19375, doi: 10.3402/tellusa.v65i0.19375, 2013.

Jonsson, A.I., de Grandpré, J., Fomichev, V.I., McConnell, J.C., Beagley, S.C.: Doubled CO_2-induced cooling in the middle atmosphere: Photochemical analysis of the ozone radiative feedback, Journal of Geophysical Research, 109, D24103, doi:10.1029/2004JD005093, 2004

Kageyama M., and co-authors: The PMIP4 contribution to CMIP6 – Part 4: Scientific objectives and experimental design of the PMIP4-CMIP6 Last

Glacial Maximum experiments and PMIP4 sensitivity experiments, Geosci. Model Dev., 10, 4035-4055, doi:10.5194/gmd-10-4035-2017, 2017.

Kinnison, D.E., Brasseur, G.P., Walters, S., Garcia, R.R. Marsh, D.R, Sassi, F., Harvey, V.L., Randall, C.E., Emmons, L., Lamarque, J.F., Hess, P., Orlando, J.J., Tie, X.X., Randall, W., Pan, L.L., Gettelman, A., Granier, C., Diehl, T., Niemeijer, Y., Simmons, A.J.: Sensitivity of chemical tracers to meteorological parameters in the MOZART-3 chemical transport model, J. Geophys. Res., 112, D20302, doi:10.1029/2006JD007879, 2007.

Lindzen, R.S.: Turbulence stress owing to gravity wave and tidal breakdown, J. Geophys. Res., 86, 9707–9714, doi:10.1029/JC086iC10p09707, 1981.

Ljungqvist, F.C., Zhang, Q., Brattström, G., Krusic, P.J., Seim, A., Li, Q., Zhang, Q., and Moberg, A.: Centennial-scale temperature change in last millennium simulations and proxy-based reconstructions, Journal of Climate, doi: 10.1175/JCLI-D-18-0525.1, 2019.

Lu, J., and Cai, M.: A new framework for isolating individual feedback processes in coupled general circulation climate model. Part I: Formulation. Climate dynamics, 32 (6), 873–885, doi:10.1007/s00382-008-0425-3, 2009.

Manabe, S., & Strickler, R. F.: Thermal equilibrium of the atmosphere with a convective adjustment. *Journal of the Atmospheric Sciences*, *21*(4), 361-385, 1964.

Marsh, D.R., Mills, M.J. Kinnison, D.E., Lamarque, J.F., Calvo, N., Polvani, L.M.: Climate change from 1850 to 2005 simulated in CESM1(WACCM), J. Climate, 26, 7372–7391, doi:10.1175/JCLI-D-12-00558.1, 2013.

Marsh, D.R., Lamarque, J.-F., Conley, A.J. and Polvani, L.M., Stratospheric ozone chemistry feedbacks are not critical for the determination of climate sensitivity in CESM1(WACCM), Geophys. Res. Lett., 43, 3928–3934, doi:10.1002/2016GL068344, 2016.

McFarlane, N.A., The effect of orographically excited wave drag on the general circulation of the lower stratosphere and troposphere, J. Atmos. Sci., 44, 1775–1800, doi:10.1175/15200469(1987)044<1775:TEOOEG>2.0.CO;2, 1987.

Neale, R., Richter, J., Park, S., Lauritzen, P., Vavrus, S., Rasch, P. and Zhang, M: The mean climate of the Community Atmosphere Model (CAM4) in forced SST and fully coupled experiments, J. Climate, 26, 5150–5168, doi:10.1175/JCLI- D-12-00236.1, 2013.

Noda, S., Kodera, K., Adachi, Y., Deushi, M., Kitoh, A., Mizuta, R., Murakami, S., Yoshida, K., Yoden, S.: Impact of interactive chemistry of stratospheric ozone on Southern Hemisphere paleoclimate simulation. Journal of

Geophysical Research: Atmospheres, 122(2), 878-895, doi:10.1002/2016JD025508, 2017.

Nowack, P.J., Abraham, N.L., Maycock, A.C., Braesicke, P., Gregory, J.M., Joshi, M.M., Osprey, A., Pyle, J.A.: A large ozone-circulation feedback and its implications for global warming assessments, Nature Climate Change, 5 (1), 41-45, 2015, doi:10.1038/NCLIMATE2451, 2015.

Nowack, P.J., Abraham, N.L., Braesicke, P. and Pyle, J.A.: The impact of stratospheric ozone feedbacks on climate sensitivity estimates. Journal of Geophysical Research: Atmospheres, 123(9), 4630-4641, doi:10.1002/2017JD027943, 2018.

Oberländer, S., Langematz, U. and Meul, S.: Unraveling impact factors for future changes in the Brewer-Dobson circulation, Journal of Geophysical Research: Atmospheres, 118, 10296-10312, doi:10.1002/jgrd.50775, 2013.

Ramaswamy, V., Collins, W., Haywood, J., Lean, J., Mahowald, N., Myhre, G., Naik, V., Shine, K.P., Soden, B., Stenchikov, G., Storelvmo, T., 2019: Radiative forcing of climate: The historical evolution of the radiative forcing concept, the forcing agents and their quantlification, and application, Meteorol. Monogr. 59, 14.1 14.99. Revell, L.E., Bodeker, G.E., Huck, P. E., Williamson, B.E. and Rozanov, E.: The sensitivity of stratospheric ozone changes through the 21st century to N_2O and CH_4. Chem. Phys., 12(23), 11309-11317, doi:10.5194/acp-12-11309-2012, 2012.

Richter, J.H., Sassi, F., Garcia, R.R.: Toward a physically based gravity wave source parameterization in a general circulation model, J. Atmos. Sci., 67, 136–156, doi:10.1175/2009JAS3112.1, 2010.

Rieger, V.S., Dietmüller, S., Ponater, M., 2017: Can feedback analysis be used to uncover the physical origin of climate sensitivity and efficacy differences? Clim. Dyn. 49, 2831-2844.

Riese, M., Ploeger, F., Rap, A., Vogel, B., Konopka, P., Dameris, M., & Forster, P. (2012). Impact of uncertainties in atmospheric mixing on simulated UTLS composition and related radiative effects. *Journal of Geophysical Research: Atmospheres*, *117*(D16).

Royer, J.F., Planton, S., Déqué, M.: A sensitivity experiment for the removal of Arctic sea ice with the French spectral general circulation model, Climate Dynamics, 5(1), 1-17, doi:10.1007/BF00195850, 1990.

Schmidt, H., Brasseur, G.P, Charron, M., Manzini, E., Giorgetta, M.A., Diehl, T., Fomichev, V., Kinnison, D., Marsh, D., Walters, S., The HAMMONIA Chemistry Climate Model: Sensitivity of the mesopause region to the 11-year solar cycle and CO2 doubling, Journal of Climate 19(16), 3903-3931, doi:10.1175/JCLI3829.1, 2006.

Shepherd, T.G.: Dynamics, stratospheric ozone and climate change, Atmosphere-Ocean, 46,1, 117-138, doi:10.3137/ao.460106, 2008.

Shepherd, T. G.: Large-scale atmospheric dynamics for atmospheric chemists. *Chemical reviews*, *103*(12), 4509-4532, 2003.

Shepherd, T.G., and McLandress, C.: A robust mechanism for strengthening of the Brewer–Dobson circulation in response to climate change: critical layer control of subtropical wave breaking. Journal of the Atmospheric Sciences, 68, 4, doi:10.1175/2010JAS3608, 2011.

Sigmond, M., Siegmund, P.C., Manzini, E. and Kelder, H.: A simulation of the separate climate effects of middle-atmospheric and tropospheric CO_2 doubling, Journal of Climate, 17(12), 2352-2367, doi:10.1175/1520-0442(2004)017<2352:ASOTSC>2.0.CO;2, 2004.

Soden, B., Held, I.M.,: An assessment of climate feedbacks in coupled ocean-atmosphere models, J. Clim. 19, 3354-3360, 2006.

Solomon, S., Rosenlof, K. H., Portmann, R. W., Daniel, J. S., Davis, S. M., Sanford, T. J., & Plattner, G. K.: Contributions of stratospheric water vapor to decadal changes in the rate of global warming. *Science*, *327*(5970), 1219-1223, 2010.

Song, X., and Zhang, G.J.: Role of climate feedback in El Niño-like SST response to global warming, J. Climate, 27, 7301–7318, doi:10.1175/JCLI-D-14-00072.1, 2014

Taylor, K.E., Stouffer R.J., and Meehl, G.: An overview of CMIP5 and the experimental design, Bull. AM. Meterorol. Soc, 93, 485-498, doi: 10.1175/BAMS-D-11-00094.1, 2012.

Taylor, P.C., Cai, M., Hu, A., Meehl, J., Washington, W. and Zhang, G.J.: A decomposition of feedback contributions to polar warming amplification, J. Climate, 26, 7023–7043, doi:10.1175/JCLI-D-12-00696.1, 2013.

Zhang, P., Wu, Y., Simpson, I.R., Smith, K.L., Zhang, X., De, B., and Callaghan, P.: A stratospheric pathway linking a colder Siberia to Barents-Kara Sea sea ice loss, Science advances, 4(7), eaat6025, doi: 10.1126/sciadv.aat6025, 2018.

Zheng, J., Zhang, Q., Li, Q., Zhang, Q. and Cai, M., Contribution of sea ice albedo and insulation effects to Arctic amplification in the EC-Earth Pliocene simulation, Clim. Past, 15, 291-305, doi:10.5194/cp-15-291-2019, 2019.

Zhu, X., Yee, J.-H., Cai, M., Swartz, W.H., Coy, L., Aquila, V., Garcia, R., Talaat, E.R.: Diagnosis of middle-atmosphere climate sensitivity by the climate feedback-response analysis method, Journal of Atmospheric Sciences, 73(1), 3-23, doi:10.1175/JAS-D-15-0013.1, 2016.